Available online at www.sciencedirect.com
SCIENCE DIRECT
Solid State Ionics 177 (2006) 429 – 436
SOLID STATE IONICS
www.elsevier.com/locate/ssi

Formation of $BaTiO_3$ thin films from (110) TiO_2 rutile single crystals and $BaCO_3$ by solid state reactions

Andriy Lotnyk *, Stephan Senz, Dietrich Hesse

Max Planck Institute of Microstructure Physics, D-06120 Halle (Saale), Germany

Received 6 July 2005; received in revised form 1 November 2005; accepted 21 December 2005

Abstract

The formation of $BaTiO_3$ thin films from (110) TiO_2 rutile single crystals and $BaCO_3$ was investigated experimentally by solid–solid and gas–solid reactions in vacuum. X-ray diffraction revealed the formation of an intermediate Ba_2TiO_4 phase before $BaTiO_3$ is formed. According to our calculations the formation of Ba_2TiO_4 is associated with a maximum decrease in the Gibbs energy at a CO_2 pressure lower than 10^{-4} mbar. Reactions at 600–900 °C showed different processes to occur in the solid–solid and gas–solid reactions. The observations are interpreted in terms of the different mass transport mechanisms involved. The results shed new light on the phase sequence during $BaTiO_3$ formation; in particular a dissociation of $BaCO_3$ prior to its participation in the reaction has become rather unlikely.

Keywords: Solid state reactions; Barium orthotitanate; Barium metatitanate; Barium carbonate; XRD analyses

1. Introduction

The perovskite-type compound $BaTiO_3$ exhibits ferroelectric ordering at temperatures below 120 °C. Ferroelectric and dielectric ceramics based on $BaTiO_3$ are widely used for high-performance multilayer ceramic capacitors (MLCCs) and thermoresistors.

The common way to produce $BaTiO_3$ ceramics from $BaCO_3$ and TiO_2 powders is to make use of solid state reactions [1–6]. The mainly adopted mechanism to explain the sequence of forming phases during calcination of $BaCO_3$ and TiO_2 powders was proposed by Beauger et al. [5,6]. The formation processes that may occur during calcination under vacuum are described as follows:

First scheme:

a) Decomposition of $BaCO_3$ according to:

$$BaCO_3 \rightarrow \text{“}BaO\text{”} + CO_2; \quad (1)$$

b) Formation of Ba_2TiO_4 by reaction between the two oxides:

$$2BaO + TiO_2 \rightarrow Ba_2TiO_4; \quad (2)$$

c) Finally, synthesis of $BaTiO_3$ according to:

$$Ba_2TiO_4 + TiO_2 \rightarrow 2BaTiO_3. \quad (3)$$

Second scheme:

(a) Decomposition of $BaCO_3$ according to reaction (1);
(b) Formation of $BaTiO_3$ by direct reaction between the oxides:

$$BaO + TiO_2 \rightarrow BaTiO_3; \quad (4)$$

(c) Formation of Ba_2TiO_4 at the expense of $BaTiO_3$ according to:

$$BaTiO_3 + BaO \rightarrow Ba_2TiO_4; \quad (5)$$

(d) Finally, the Ba_2TiO_4 reacts with the TiO_2 nucleus to form $BaTiO_3$ according to reaction (3).

* Corresponding author. Tel.: +49 345 5582 692; fax: +49 345 5511223.
E-mail address: lotnyk@mpi-halle.de (A. Lotnyk).

0167-2738/$ - see front matter © 2006 Elsevier B.V. All rights reserved.
doi:10.1016/j.ssi.2005.12.027

However, the experimental observations of Beauger et al. [5,6] did not allow to make a choice between these two schemes. Thus, the mechanism of $BaTiO_3$ formation from $BaCO_3$ and TiO_2 is still open. Hence, the selection of this rather complex system for a phase formation study in model experiments using single crystals as one reactant [7] should be a way to gain a better understanding of the process.

Tochitsky and Romanova [8] investigated solid state reactions in the multicomponent thin film systems TiO_2/BaO, $TiO_2/BaCO_3$, TiO_2/PbO, and TiO_2/Bi_2O_3. The thin film systems were prepared by a layer-by-layer thermal evaporation of metals onto alkali halide single crystal substrates in a vacuum of about 10^{-5} mbar followed by annealing in an O_2 ambient. The authors found that in the $TiO_2/BaCO_3$ system after annealing at 500–800 °C only the $BaTiO_3$ compound formed.

On the other hand, a topotaxial reaction can take place between $BaTiO_3$ and TiO_2 as shown in Ref. [9]. In contrast, topotaxy between TiO_2 and Ba_2TiO_4 has not been reported yet.

Therefore, the aim of the present study is to experimentally investigate the phase formation sequence during $BaTiO_3$ formation in model experiments. Titanium dioxide (rutile) (110) single crystals (the thermodynamically most stable crystal face) are used as substrates to provide a model system. The solid state reactions of the latter with $BaCO_3$ (solid and vapour, respectively) in high vacuum, and the orientation relationship of the final products with respect to the substrate are studied.

2. Experimental

In the reaction experiments, polished (110) surfaces of commercial rutile TiO_2 (T) single crystals (CrysTec GmbH, Berlin, Germany) were subjected to $BaCO_3$ vapour. The latter was obtained by electron-beam evaporation of a $BaCO_3$ powder target in a high-vacuum system. Before the experiments the (110) TiO_2 substrates were annealed in air at 1100 °C for 1 h. After this heat treatment the substrate surface involves terraces of about 150 nm in width with ordered steps of about 0.6 nm in height as shown by AFM.

The base pressure of the vacuum system was $(1-2)\times10^{-5}$ mbar. During deposition, pure O_2 was introduced to establish a pressure of 1×10^{-4} mbar. The deposition rate (0.08 nm/s) and the thickness of the thin film (about 100 nm) were monitored in situ by a quartz microbalance. The substrates were heated in a tube furnace from 300 to 500 °C during deposition, followed by a solid–solid reaction at 575–900 °C between $BaCO_3$ and TiO_2 for 30 min; for the gas–solid reaction, the substrates were heated from 575 to 900 °C directly during deposition. The temperatures were measured by a Pt/PtRh10 thermocouple. After the solid state reactions the samples were kept in the vacuum chamber and allowed to cool to room temperature.

The phases present in the thin films after the reaction, and their orientation relationships were investigated by X-ray diffraction (XRD, Philips Xpert MRD) with CuK_α radiation. $\theta-2\theta$ and 2θ measurements were performed to identify the oriented and polycrystalline reaction products. The $\theta-2\theta$ scans were taken after optimising φ and ψ for the (220) substrate plane. Pole figures (center: $\psi=0°$, rim: $\psi=90°$) were taken with ψ steps of 2° to determine the crystallographic orientation of the thin films relative to the rutile substrate. $\psi=0°$ in all pole figures corresponds to the planes of the thin film being parallel to the substrate surface whereas $\psi=90°$ corresponds to the planes of the thin film being perpendicular to the substrate surface.

3. Results

3.1. Phase formation

3.1.1. Solid–solid reaction

The presence of $BaCO_3$ (JCPDS 45-1471, barium carbonate, BC), Ba_2TiO_4 (JCPDS 38-1481, barium orthotitanate, B2T) and $BaTiO_3$ (JCPDS 89-2475, barium metatitanate, BT) phases depending on the reaction temperature was investigated by XRD. After deposition at a temperature between 300 and 500 °C a single $BaCO_3$ phase was observed. At 500 °C the orientation relationship between the barium carbonate and the substrate is well-defined as indicated by the XRD $\theta-2\theta$ scan (Fig. 1b) and a pole figure (Fig. 2). Most of the solid–solid reactions were conducted using $BaCO_3$ layers grown at 500 °C.

A deposition at 500 °C followed by solid–solid reaction at ≈575–600 °C for 30 min produced a single Ba_2TiO_4 phase (Fig. 1c). The Ba_2TiO_4 had an orthorhombic structure as indicated by pole figure analyses.

In order to evaluate the rate of the solid–solid reaction, the $BaCO_3-TiO_2$ system was annealed at constant temperature (≈575–600 °C) for different length of times. The reaction proceeds from a $BaCO_3$ layer to a mixture of $BaCO_3$ and Ba_2TiO_4. As soon as all the $BaCO_3$ has been consumed, the film consists only of Ba_2TiO_4. Both $BaCO_3$ and Ba_2TiO_4 phases were found immediately after heating the sample up to ≈575 °C (holding time null minutes) while only the Ba_2TiO_4 phase was observed after annealing at 600 °C for one minute. The effect of a short holding time is mainly given by the heating during ramp up and ramp down (≈5 K/min). Increasing the reaction time up to 180 min at 600 °C resulted, together with the Ba_2TiO_4 phase, in the formation of $BaTiO_3$.

The reaction at temperatures between 625 and 825 °C leads to the formation of both Ba_2TiO_4 and $BaTiO_3$ phases (Fig. 1d, e). The barium orthotitanate was found to be a very unstable compound and to decompose entirely after a storage for two weeks in air, most probably by reaction with H_2O and CO_2 (see Fig. 3, the unidentified peaks at 2θ ≈25.1° and 25.6° are assumed to arise from barium hydroxide hydrate (JCPDS 77-2334)). This observation is in good agreement with the data obtained in Refs. [10,11]. XRD pole figure measurements of the sample prepared after heating at 850 °C for 30 min showed the formation of $BaTiO_3$ without any evidence of remaining Ba_2TiO_4. After reaction for a short time (holding time null minutes at 850 °C) two phases (Ba_2TiO_4 and $BaTiO_3$) were identified. The solid state

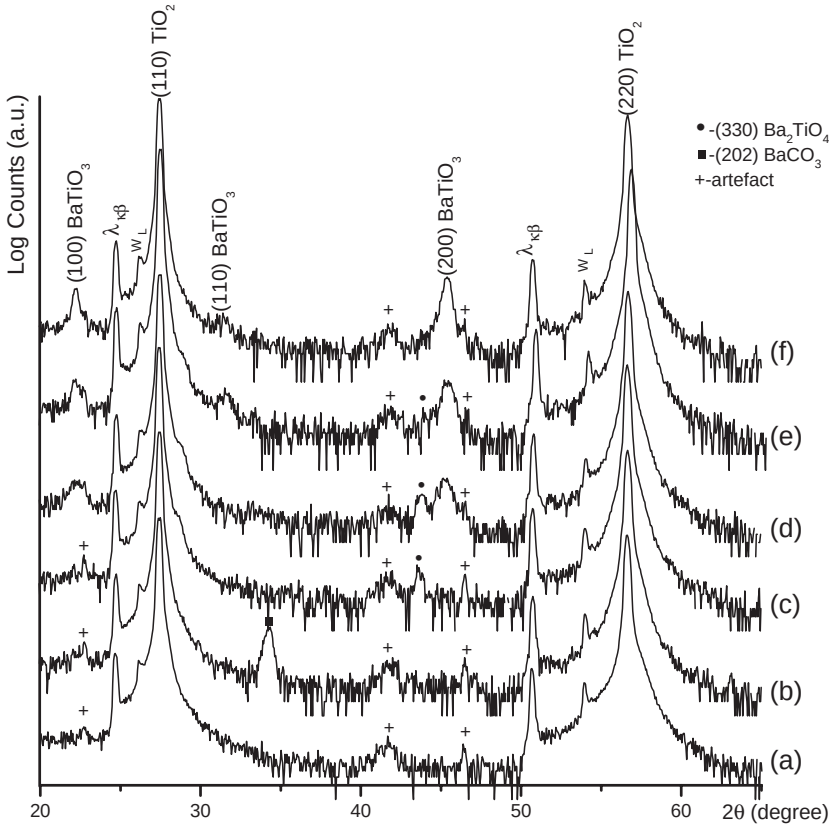

Fig. 1. XRD $2\theta-\theta$ scans for: (a) a virgin rutile substrate, (b) a thin film prepared after deposition at 500 °C followed by solid state reaction at (c) 600 °C, (d) 700 °C, (e) 800 °C, and (f) 900 °C.

reaction at 900 °C leads to the formation of $BaTiO_3$ (Fig. 1f). Additionally, the presence of Ti-rich phases was observed by pole figure measurements (not shown). It should be noted that after reaction at this temperature the samples became blue in colour. As was reported earlier [12], heating TiO_2 crystals in vacuum or under reducing conditions results in oxygen losses and corresponding change of the colour from yellowish to blue. The formation of the Ti-rich phase may thus be a result of a joint out-diffusion of oxygen and titanium from the substrate into the $BaTiO_3$ film.

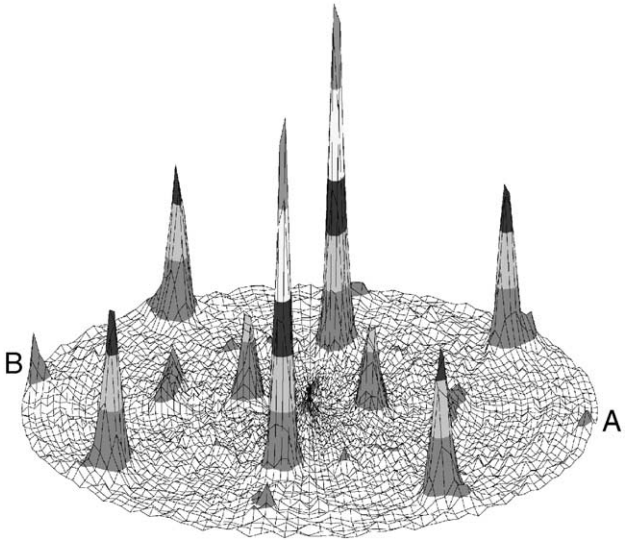

Fig. 2. $BaCO_3$ (111) ($2\theta=23.9°$) pole figure of a sample deposited at 500 °C. The positions of marks A and B in all pole figures are corresponding to the φ values of the (001) and (00$\bar{1}$) substrate planes, respectively.

3.1.2. Gas–solid reaction

The gas–solid experiments showed a reaction process that is similar to the solid–solid reaction with a shift of the temperatures of $BaTiO_3$ formation.

At a reaction temperature of ≈575 °C, only the Ba_2TiO_4 phase was identified, and between 600 and 850 °C two phases (Ba_2TiO_4 and $BaTiO_3$) were formed in contrast to the solid–solid reaction. But at 600 °C the $BaTiO_3$ phase is contained in the thin film in a small amount only as shown by the very weak intensity in the pole figures (not shown). As in the solid–solid reaction, the barium orthotitanate obtained after gas–solid reaction was also found to decompose when exposed to air for two weeks. Experiments at 900 °C show the presence of $BaTiO_3$ (see Fig. 4) and a Ti-rich phase (detected by pole figures) in the thin film.

3.2. Orientation relationships

3.2.1. Orientation of $BaCO_3$

The barium carbonate formed with a well-defined orientation with respect to the TiO_2 substrate. But the orientation relationship of the $BaCO_3$ phase was strongly dependent on the substrate temperature. Thus, at a substrate temperature of

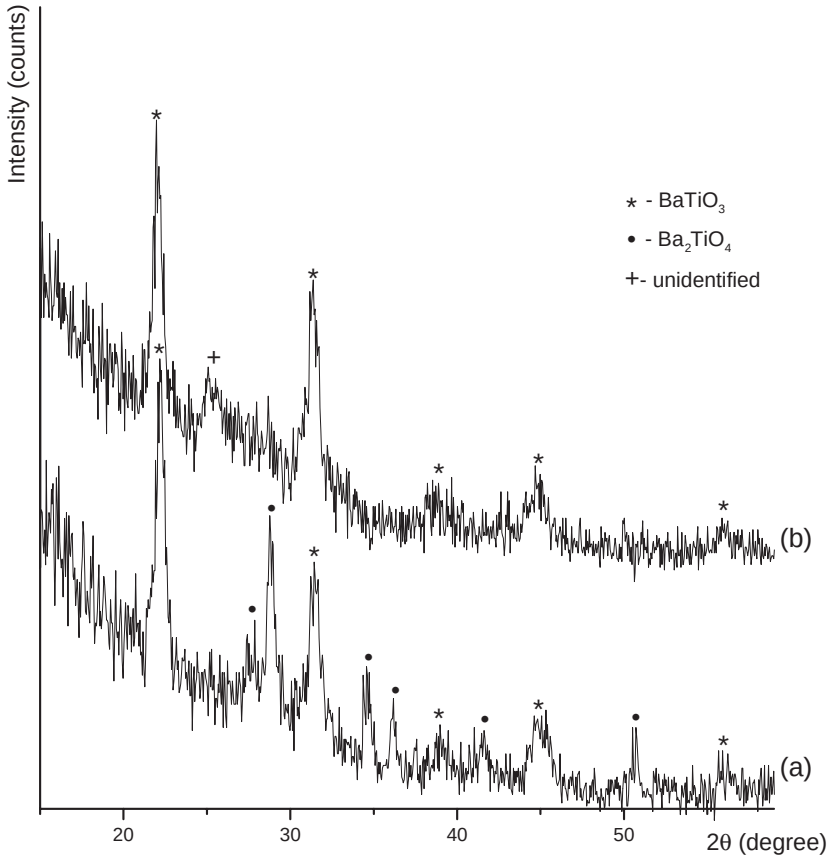

Fig. 3. XRD 2θ scan of a sample deposited at 500 °C followed by solid state reaction at 700 °C: a) as produced; b) after a storage for two weeks in air.

300 °C the XRD $\theta-2\theta$ results indicate that (111) BC||(110) T. XRD pole figure measurements recorded at 23.89° and 41.88° show, however, that no well-defined azimuthal orientation can be found at this temperature.

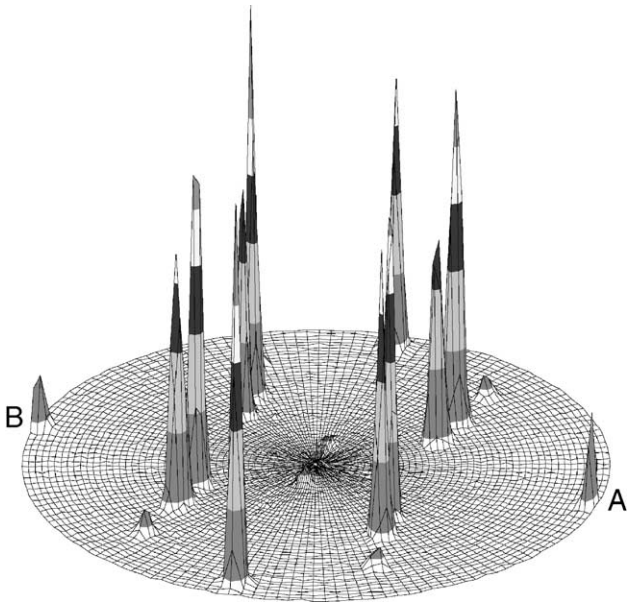

Fig. 4. $BaTiO_3$ pole figure of a sample after gas–solid reaction at 900 °C. The peaks are situated at $\psi=11°$, 40°, 50°, 70°, 82° and 90°.

At 400 °C, $BaCO_3$ is crystallographically oriented according to the relation:

main $(101)\mathrm{BC}\,||\,(110)\mathrm{T};\,[010]\mathrm{BC}\,||\,[001]\mathrm{T},$

minor $(100)\mathrm{BC}\,||\,(110)\mathrm{T};\,[01\bar{1}]\mathrm{BC}\,||\,[001]\mathrm{T}.$

Remarkably, the XRD pole figures display rather broad reflections of $BaCO_3$ both in φ and ψ directions (not shown). Fig. 1b indicates that at a substrate temperature of 500 °C (202) BC||(110) T. The in-plane orientation was determined by pole figures taken at 23.9°, 24.2° and 34.3° (one of them is shown in Fig. 2) and a φ scan of the TiO_2 (200) reflection taken at $\psi=45°$ (not shown). The φ positions corresponding to the (001) and (00$\bar{1}$) substrate planes are denoted "A" and "B", respectively (see Fig. 2). The main orientation relationship at 500 °C was derived as:

$(101)\mathrm{BC}\,||\,(110)\mathrm{T};\,[\bar{1}01]\mathrm{BC}\,||\,[001]\mathrm{T}.$

A second orientation relation was determined as:

$(21\bar{1})\mathrm{BC}\,||\,(110)\mathrm{T};\,[2\bar{3}1]\mathrm{BC}\,||\,[001]\mathrm{T}.$

3.2.2. Orientation of Ba_2TiO_4

The orientation of Ba_2TiO_4 after the solid–solid reaction was strongly dependent on the orientation quality of $BaCO_3$.

A deposition of $BaCO_3$ at 300 °C followed by solid–solid reaction at 575–700 °C for 30 min produced Ba_2TiO_4 with a low orientation quality (pole figures not shown). In contrast, a

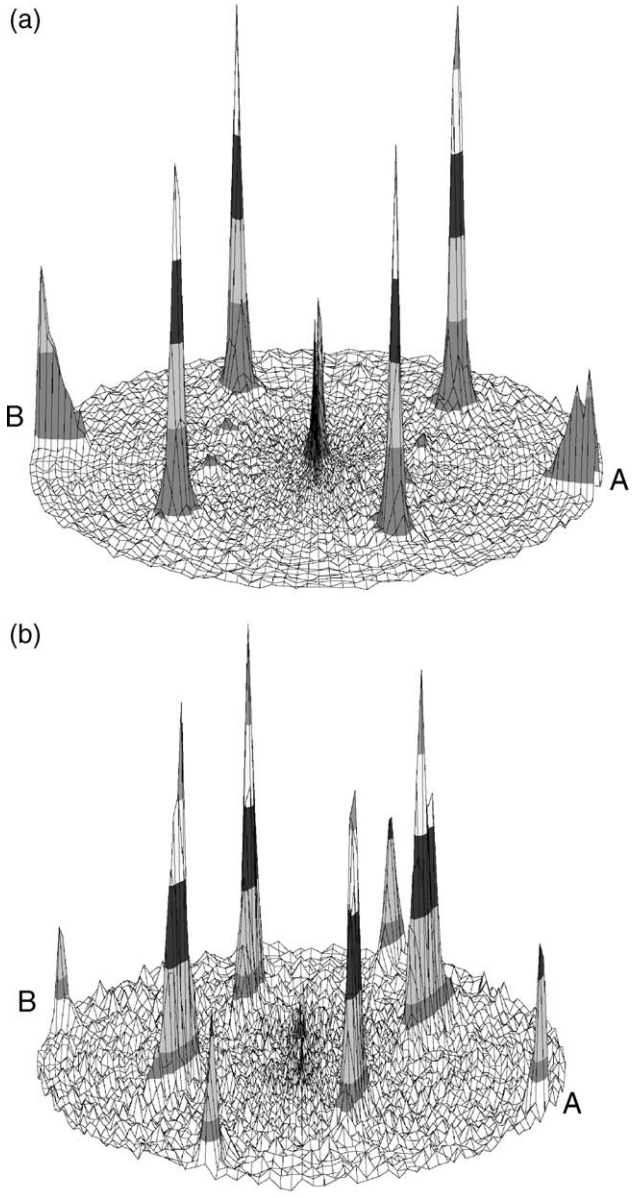

Fig. 5. X-ray pole figures of a sample prepared after solid state reaction at 700 °C: (a) $2\theta = 29.24°$ (Ba_2TiO_4 {031}/{002} family), peaks are situated at $\psi = 0°$, 60° and 90°; (b) $2\theta = 31.4°$ ($BaTiO_3$ {101} family), peaks are situated at $\psi = 45°$ and $\psi = 90°$.

deposition of $BaCO_3$ at 500 °C followed by solid–solid reaction at 575–850 °C for 30 min produced a well-oriented Ba_2TiO_4. The peak at $2\theta = 43.8°$ in Fig. 1c, d and e is from (330) Ba_2TiO_4. All results of solid–solid reactions presented in this paper use a $BaCO_3$ thin film deposited at 500 °C. Several pole figures were recorded at different 2θ values to find out which plane of Ba_2TiO_4 is parallel to the TiO_2 substrate. Fig. 5a shows a pole figure taken at $2\theta = 29.24°$ (Ba_2TiO_4 (031)/(002)) of the sample prepared after solid–solid reaction at a temperature of 700 °C. The orientation relationship of Ba_2TiO_4 with respect to the (110) rutile surface was found as follows:

$$(110)\mathrm{B2T}\,||\,(110)\mathrm{T};\ [001]\mathrm{B2T}\,||\,[001]\mathrm{T}.$$

This orientation relationship was also found for the samples prepared after the reaction at temperatures between 575 and 850 °C.

After a gas–solid reaction, the orientation relationship of the Ba_2TiO_4 phase is different compared to the solid–solid reactions. Fig. 6 shows a pole figure taken at $2\theta = 29.24°$ of the sample prepared after gas–solid reaction at a substrate temperature of 700 °C. The orientation relationship of Ba_2TiO_4 with respect to the (110) rutile surface was found as follows:

$$(100)\mathrm{B2T}\,||\,(110)\mathrm{T};\ [001]\mathrm{B2T}\,||\,[001]\mathrm{T}.$$

This orientation relationship was also observed for the samples prepared at 575–700 °C.

At a substrate temperature of 800 °C the reflections of the Ba_2TiO_4 phase in the pole figures are broad in φ and ψ directions and, thus, no well-defined orientation can be deduced.

3.2.3. Orientation of $BaTiO_3$

In this part we will present first the orientation relations of $BaTiO_3$ grains after gas–solid reaction because their tilt distribution is sharp compared to the solid–solid reaction.

A pole figure taken at $2\theta = 31.4°$ for the sample prepared after gas–solid reaction at 900 °C is presented in Fig. 4. The peaks from the $BaTiO_3$ {101} family in Fig. 4 are sharp and strong, indicating the growth of $BaTiO_3$ grains with well-defined orientation. The orientation relationships of $BaTiO_3$ were identified as:

$$\mathrm{main}(700-900°\mathrm{C})\quad (119)\mathrm{BT}\,||\,(110)\mathrm{T};\ [1\bar{1}0]\mathrm{BT}\,||\,[001]\mathrm{T},$$

$$\mathrm{minor}(800-900°\mathrm{C})\quad (331)\mathrm{BT}\,||\,(110)\mathrm{T};\ [1\bar{1}0]\mathrm{BT}\,||\,[001]\mathrm{T}.$$

Both orientations can be understood as a result of a systematic tilt around a unique tilt axis starting from low index orientations with (001) BT‖(110) T and (110) BT‖(110) T, respectively. The common tilt axis is $[1\bar{1}0]$ BT‖[001] T.

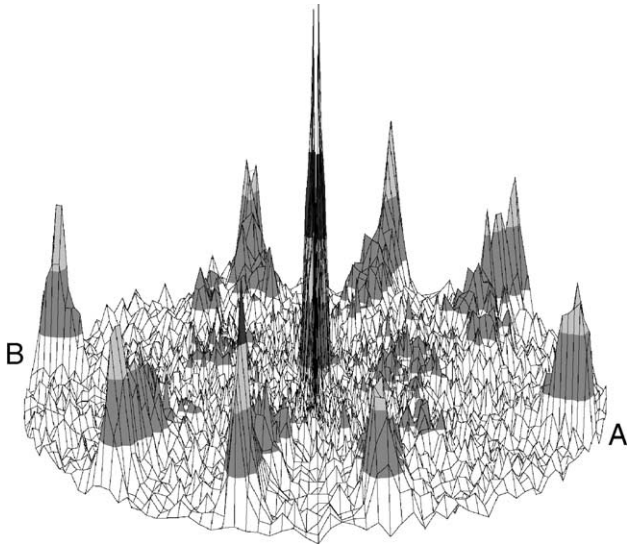

Fig. 6. X-ray diffraction pole figure of the Ba_2TiO_4 phase formed after gas–solid reaction at $T = 700$ °C. The peaks are situated at $\psi = 0°$ and 90°.

Table 1
Orientation relationships and misfit values between product phases and the (110) TiO_2 substrate

Phase	T, °C	Orientation relationship			Misfit	
		No	Plane	Direction	Film plane ∥ (001) T	Film plane ∥ (1$\bar{1}$0) T
$BaCO_3$	400	1	(101) BC∥(110) T	[010] BC∥[001] T	(010), +79.6%	($\bar{1}$02), +12.7%
		2	(100) BC∥(110) T	[0$\bar{1}$1] BC∥[001] T	(0$\bar{1}$3), −12.4%	(011), +40.5%
	500	3	(101) BC∥(110) T	[$\bar{1}$01] BC∥[001] T	($\bar{1}$02), +23.7%	(010), +63.6%
		4	(21$\bar{1}$) BC∥(110) T	[2$\bar{3}$1] BC∥[001] T	(1$\bar{1}$1), +25.8%	(013), −20.2%
Ba_2TiO_4	ss 600–850	5	(110) B2T∥(110) T	[001] B2T∥[001] T	(001), >100%	($\bar{1}$20), +33.7%
	gs 600–700	6	(100) B2T∥(110) T			(010), >100%
$BaTiO_3$	ss 700	7	(001) BT∥(110) T	[1$\bar{1}$0] BT∥[001] T	(1$\bar{1}$0), −4.1%	(1$\bar{1}$0), −12.7%
	ss 800–900	8	(110) BT∥(110) T			(001), +23.4%
	or	9	(119) BT∥(110) T			(99$\bar{2}$), >100%
	gs 700–900	10	(331) BT∥(110) T			(11$\bar{6}$), >100%

After the solid–solid reaction, the $BaTiO_3$ grains grown on (110) rutile show similar orientations. A pole figure after solid–solid reaction at 700 °C is presented in Fig. 5b. The figure displays extended reflections of the $BaTiO_3$ {101} family with a shape like a fin, which means that the $BaTiO_3$ film consists of several kinds of tilted grains with a common tilt axis. For this temperature most of the $BaTiO_3$ grains were grown with a mean orientation:

$$(001)\mathrm{BT}\,||\,(110)\mathrm{T};\,[1\bar{1}0]\mathrm{BT}\,||\,[001]\mathrm{T}.$$

With increasing temperature the number of tilted grains is increasing with systematic tilting from (001) BT∥(110) T towards (119) BT∥(110) T. After reaction at 800–900 °C XRD θ–2θ scans (Fig. 1e and f) and pole figure measurements (not shown) revealed additional minor orientations of $BaTiO_3$ such as (110) BT∥(110) T and (331) BT∥(110) T. In contrast to the formation of Ba_2TiO_4, $BaTiO_3$ formed also with (001) BT∥(110) T if a $BaCO_3$ film with low orientation quality grown at 300 °C was used.

All the determined orientation relationships between the product phases and the substrate for the solid–solid (ss) and the gas–solid reaction (gs) are listed in Table 1.

4. Discussion

4.1. Phase formation

A comparison of phase formation and orientation relationships in the solid–solid and gas–solid reactions enables us to discuss the mechanisms of $BaTiO_3$ and Ba_2TiO_4 formation. Notably, the processes to be considered occur under vacuum lower than 1×10^{-4} mbar.

In the solid–solid reactions the single intermediate Ba_2TiO_4 compound forms at the beginning of heating by reaction between barium carbonate grains and rutile single crystal. Whether step a) of the reaction according to Eq. (1) is really occurring is doubtful. The time required for the formation of Ba_2TiO_4 is low compared to the decomposition time of $BaCO_3$ reported by Judd and Pope [13] or by L'vov [14]. Thus we rather expect a direct reaction of $BaCO_3$ with TiO_2. It was shown that both $BaCO_3$ and Ba_2TiO_4 phases were found immediately after the reaction at 575 °C (holding time null minutes). For short reaction times at this temperature, a decomposition of $BaCO_3$ into BaO and CO_2 and a subsequent reaction of BaO with TiO_2 are unlikely. For the influence of the Gibbs energy in dependence on the CO_2 pressure, see below.

In the gas–solid reaction we expect barium oxide and titanium oxide as the reacting species. $BaCO_3$ evaporates by decomposition, the vapour consisting of BaO and CO_2. Thus first BaO is condensing on the surface. The formation of $BaCO_3$ by reaction with CO_2 vapour at a temperature of 575 °C is suppressed by a positive value of the Gibbs energy when the partial pressure of CO_2 is lower than 1×10^{-5} mbar (estimation see below). At a temperature of 500 °C the Gibbs energy of $BaCO_3$ formation is negative, consistent with the observation of $BaCO_3$ film growth.

According to our calculations, the formation of barium orthotitanate is accompanied by a maximum decrease in Gibbs energy. The results of these calculations are presented in Table 2. The ΔG^0 (standard Gibbs energy) values were taken from Ref. [15] at $T=1000$ K ($P_{CO_2}=1$ bar) where two phases (Ba_2TiO_4 and $BaTiO_3$) were identified. The values of ΔG^{air} and ΔG^{vac} were calculated for reactions occurring in air (where $P_{CO_2}=0.3$ mbar) and in vacuum (the absolute background

Table 2
Standard Gibbs free energy of reactions (ΔG^0, $P_{CO_2}=1$ bar) and the change in Gibbs free energy during reactions in air (ΔG^{air}, $P_{CO_2}=0.3$ mbar) and under vacuum (ΔG^{vac}, $P_{CO_2}=1\times10^{-5}$ mbar) at $T=1000$ K

N	Reaction	ΔG^0, kJ/mol	ΔG^{air}, kJ/mol	ΔG^{vac}, kJ/mol
1	$2BaCO_3 + TiO_2 \rightarrow Ba_2TiO_4 + 2CO_2$	+3.7	−131.1	−302.5
2	$BaCO_3 + TiO_2 \rightarrow BaTiO_3 + CO_2$	−48.7	−116.1	−201.8
3	$BaCO_3 + BaTiO_3 \rightarrow Ba_2TiO_4 + CO_2$	+52.1	−15.3	−101
4	$BaCO_3 \rightarrow BaO + CO_2$	+101.8	+34.4	−51.3

pressure of the vacuum system was $\leq 2\times10^{-5}$ mbar, thus the partial pressure of CO_2 during our experiments was lower than 1×10^{-5} mbar), respectively. In reaction nos (1)–(4) (see Table 2), the chemical potential of CO_2 gas depends on its partial pressure and is described by [16]:

$$\mu_{CO_2} = g^0_{CO_2} + RT\ln P_{CO_2},$$

where μ is the chemical potential of CO_2 and g_{CO_2} is the molar Gibbs free energy of CO_2. For one mole, $\mu_{CO_2}=G_{CO_2}$ and $g^0_{CO_2}=G^0_{CO_2}$. As can be seen from Table 2, reaction no (4) in vacuum is relatively unfavourable compared to reaction nos (1) or (2) due to an only small decrease in the Gibbs energy. From a thermodynamical point of view, reactions nos (1), (3) and (4 at a pressure of 1 bar and reaction no (4) in air (T=1000 K) are hindered by a positive value of the Gibbs energy and can thus be observed only under low pressure [2].

Although thermodynamics describes whether or not a solid state reaction will occur, it does not give any information on the kinetics of such reactions. Thin film reactions are determined by processes at the reaction fronts, or by nucleation phenomena, whereas reactions in the bulk are controlled by diffusion. In our case, the initial formation of $BaTiO_3$ during the solid–solid reaction at T=575–600 °C may have been hindered due to a nucleation barrier, so that the first phase forming was Ba_2TiO_4. In the gas–solid reaction, surface diffusion may be predominant, and independent nucleation events at surface defects may have occurred. Thus, a similar nucleation probability of $BaTiO_3$ and Ba_2TiO_4 in the gas–solid reaction may have facilitated the initial formation of both phases.

We can assume different formation mechanisms of Ba_2TiO_4 and $BaTiO_3$ based on the differences in the orientations of both phases in dependence on the orientation of $BaCO_3$. The orientation of Ba_2TiO_4 is strongly dependent on the orientation of $BaCO_3$, while the orientation of $BaTiO_3$ grains is independent of the $BaCO_3$ orientation. The formation of Ba_2TiO_4 might be the result from diffusion of Ti ions into the $BaCO_3$ matrix. In contrast, $BaTiO_3$ grains might be formed by diffusion of Ba ions into TiO_2.

The formation temperatures of Ba_2TiO_4 and $BaTiO_3$ under our experimental conditions were substantially lower than those in bulk ceramic systems [17]. For an explanation one should consider that in ceramic samples the grain sizes (about 2–5 μm) are much larger compared to grain sizes in thin films (about 20–50 nm), so that mass transport in bulk ceramics is not sufficient at low temperatures.

4.2. Orientation relationships

Comparing the orientations of the phases formed on (110) TiO_2 the similarities and differences become obvious. The orientations of $BaTiO_3$ grains after two types of solid state reactions have similar features but with different sharpness of the tilt distributions. In contrary, the Ba_2TiO_4 grains after solid–solid reaction show another orientation compared to the gas–solid reaction. This difference might be caused by different nucleation mechanisms. During the solid–solid reaction Ti ions seem to be diffusing into the $BaCO_3$ film. The gas–solid reaction starts by surface diffusion of BaO on the TiO_2 substrate. The relations [1$\bar{1}$0] BT‖[001] T and [001] B2T‖[001] T are observed under different reaction conditions. This means that the [001] TiO_2 axis is the tilt axis for compounds grown on (110) TiO_2, independent of their crystallographic structure.

From Table 1 we see that the interplanar distances of barium carbonate and barium orthotitanate do not fit the respective ones in rutile in both directions (items 1–6). One interplanar distance of $BaTiO_3$ matches with one of TiO_2 in the [001] TiO_2 direction giving a rather low lattice misfit of −4.1% (items 7–10) but no match occurs in the perpendicular direction.

To explain the occurrence of interfaces with a rather large lattice misfit in Table 1, a near coincidence site lattice (NCSL) model [18,19] was applied for the thin films on the (110) rutile substrate. The model is a generalisation of the coincidence site lattice (CSL) theory. For heteroepitaxial interfaces, the non-commensurate relationship between the lattice parameters of the two materials means that exact coincidence cannot be found and hence a lattice misfit or “near coincidence” is introduced. We consider the interface between two crystalline materials with lattice parameters a and b, respectively, as a two-dimensional rectangular lattice. Exact coincidence occurs when $n\cdot a = m\cdot b$, where m and n are integers. The misfit is given by

$$F = 2\cdot(n\cdot a - m\cdot b)/(n\cdot a + m\cdot b).$$

In the NCSL theory, the smaller the misfit and the higher the periodicity (low m, n) are, the lower is the interfacial energy. We calculated NCSL misfits for all index combinations ($-9\leq$(h, k, l)$\leq+9$) using a computer program written in the Free Pascal programming language [20]. Although the observed orientation relations between $BaCO_3$ and (110) TiO_2 (Table 3)) can be matched by choosing $n\leq8$, $m\leq13$ and $|F|\leq1\%$, there are much better matching orientation relations with m$\leq$3, n$\leq$2 and |F|$\leq$0.9% found by our program. One example is (02$\bar{5}$) BC‖(001) T (n_1=2, m_1=1, F_1=−0.04%) and (100) BC‖(1$\bar{1}$0) T (n_2=1, m_2=2, F_2=−0.9%). Clearly, the NCSL theory based on a simple geometrical criterion cannot select the observed orientations of $BaCO_3$ out of a larger set of low-misfit solutions.

As was mentioned above, the interplanar distances of $BaTiO_3$ (items 7–10 in Table 1) do not fit those of TiO_2 in

Table 3
The misfit values between product phases and rutile substrate calculated by NCSL theory

Phase	No	Film plane ‖ (001) T			Film plane ‖ (1$\bar{1}$0) T		
		n_1	m_1	F_1, %	n_2	m_2	F_2, %
$BaCO_3$	1	5	9	−0.2	8	9	+0.2
	2	8	7	+0.04	5	7	+0.4
	3	4	5	−1	8	13	+0.7
	4	4	5	+0.5	5	4	−0.2
Ba_2TiO_4	5	1	2	+3.1	3	4	+0.4
	6	1	2	+3.1	3	10	−2.6
$BaTiO_3$	7	1	1	−4.1	8	7	−0.2
	8				4	5	−1.2
	9				10	1	−4.3
	10				5	1	+0.3

the [1$\bar{1}$0] TiO_2 direction but are well matched in the [001] TiO_2 direction. The non-matching orientation relations of $BaTiO_3$ can be matched using the NCSL model (see Table 3) with $n \leq 10$, $m \leq 7$ and $|F| \leq 4.3\%$. The non-matching orientation relations for Ba_2TiO_4 in the [001] and [1$\bar{1}$0] TiO_2 directions (items 5–6 in Table 1) are fitted by choosing $n \leq 3$ and $m \leq 10$ with $|F| \leq 3.1\%$ (Table 3) in the NCSL model. The NCSL theory seems to be able to describe why a particular observed orientation relationship is a good one, but without predictive power.

5. Conclusions

The formation of $BaTiO_3$ from $BaCO_3$ and (110) rutile single crystals has been studied experimentally under vacuum by solid state reactions. A dissociation of $BaCO_3$ prior to its participation in the reaction is rather unlikely. The formation of $BaTiO_3$ was always preceded by an intermediate Ba_2TiO_4 compound that formed by direct reaction between $BaCO_3$ and rutile single crystals. This is in contrast to the model of Beauger et al. [5,6]. The barium orthotitanate was found to be an unstable compound and to decompose entirely after a storage of two weeks in air, most probably by reaction with H_2O and CO_2.

According to our calculations the formation of the intermediate phase Ba_2TiO_4 is associated with a maximum decrease in the Gibbs energy. The formation temperatures of Ba_2TiO_4 and $BaTiO_3$ under our experimental conditions were substantially lower than those in bulk ceramic samples. Different formation mechanisms of Ba_2TiO_4 and $BaTiO_3$ are assumed. The formation of Ba_2TiO_4 is discussed as diffusion of Ti ions into $BaCO_3$, while $BaTiO_3$ might be formed by diffusion of Ba ions into TiO_2.

Different orientation relations have been found for $BaCO_3$, Ba_2TiO_4 and $BaTiO_3$ depending on the reaction conditions, all of which imply, however, a common [001] TiO_2 tilt axis. Although the observed orientations of $BaCO_3$ on (110) TiO_2 are in principal accordance with an NCSL model, this model did not allow to uniquely define the observed orientations. The orientation relations of the Ba_2TiO_4 and $BaTiO_3$ phases, however, can be explained in terms of a good lattice fit (at least in one direction). A more detailed discussion of the type of the diffusing species and crystallographic details of these reactions, as well as related TEM investigations, is in progress.

Acknowledgement

Work supported by Deutsche Forschungsgemeinschaft (DFG) via SFB 418 at Martin-Luther-Universität Halle–Wittenberg.

References

[1] D.E. Rase, R. Roy, J. Am. Ceram. Soc. 38 (1955) 102.
[2] M. Cournil, M. Soustelle, G. Thomas, Oxid. Met. 13 (1979) 77.
[3] M. Cournil, M. Soustelle, G. Thomas, Oxid. Met. 13 (1979) 89.
[4] J.C. Mutin, J.C. Niepce, J. Mater. Sci. Lett. 3 (1984) 591.
[5] A. Beauger, J.C. Mutin, J.C. Niepce, J. Mater. Sci. 18 (1983) 3041.
[6] A. Beauger, J.C. Mutin, J.C. Niepce, J. Mater. Sci. 18 (1983) 3543.
[7] S. Senz, A. Graff, W. Blum, D. Hesse, J. Am. Ceram. Soc. 81 (1998) 1317.
[8] E.I. Tochitsky, N.I. Romanova, Thin Solids Films 110 (1983) 55.
[9] Y. Suyama, Y. Oda, A. Kato, Chem. Lett. 8 (1979) 987.
[10] K.-H. Felgner, T. Müller, H.T. Langhammer, H.-P. Abicht, Mater. Lett. 58 (2004) 1943.
[11] S.J. Lee, M.D. Biegalski, W.M. Kriven, J. Mater. Res. 14 (1999) 3001.
[12] Y.W. Chung, W.J. Lo, G.A. Somorjai, Surf. Sci. 64 (1977) 588.
[13] M.D. Judd, M.I. Pope, J. Therm. Anal. 4 (1972) 31.
[14] B.V. L'vov, Thermochim. Acta 386 (2002) 1.
[15] I. Barin, Thermochemical data of pure substances. VCH Verlagsgesellschaft, Weinheim, 1995, p.p. 133, 148, 157–158, 404, 1692.
[16] N.K. Adam, Physical Chemistry, Oxford University Press, London, 1962, p. 289.
[17] J.J. Ritter, R.S. Roth, J.E. Blendell, J. Am. Ceram. Soc. 69 (1986) 155.
[18] H. Grimmer, W. Bollmann, D.H. Warrington, Acta Crystallogr. 30 (1974) 197.
[19] T.X.T. Sayle, C.R.A. Catlow, D.C. Sayle, S.C. Parker, J.H. Harding, Philos. Mag., A 68 (1993) 565.
[20] www.freepascal.org.